2013

# Role of MerH in mercury resistance in the archaeon *Sulfolobus solfataricus*

James Schelert
*University of Nebraska - Lincoln*

Deepak Rudrappa
*University of Nebraska–Lincoln*

Tyler Johnson
*University of Nebraska–Lincoln*

Paul H. Blum
*University of Nebraska - Lincoln*, pblum1@unl.edu

PMCID: PMC3709690

*Microbiology* (2013), **159**, 1198–1208 DOI 10.1099/mic.0.065854-0

# Role of MerH in mercury resistance in the archaeon *Sulfolobus solfataricus*

James Schelert,† Deepak Rudrappa, Tyler Johnson and Paul Blum

School of Biological Sciences, University of Nebraska–Lincoln, Lincoln, NE 68508, USA

Correspondence
Paul Blum
pblum1@unl.edu

Received 4 January 2013
Accepted 19 April 2013

*Crenarchaeota* include extremely thermoacidophilic organisms that thrive in geothermal environments dominated by sulfidic ores and heavy metals such as mercury. Mercuric ion, Hg(II), inactivates transcription in the crenarchaeote *Sulfolobus solfataricus* and simultaneously derepresses transcription of a resistance operon, *merHAI*, through interaction with the MerR transcription factor. While mercuric reductase (MerA) is required for metal resistance, the role of MerH, an adjacent small and predicted product of an ORF, has not been explored. Inactivation of MerH either by nonsense mutation or by in-frame deletion diminished Hg(II) resistance of mutant cells. Promoter mapping studies indicated that Hg(II) sensitivity of the *merH* nonsense mutant arose through transcriptional polarity, and its metal resistance was restored partially by single copy *merH* complementation. Since MerH was not required *in vitro* for MerA-catalysed Hg(II) reduction, MerH may play an alternative role in metal resistance. Inductively coupled plasma-mass spectrometry analysis of the MerH deletion strain following metal challenge indicated that there was prolonged retention of intracellular Hg(II). Finally, a reduced rate of *mer* operon induction in the *merH* deletion mutant suggested that the requirement for MerH could result from metal trafficking to the MerR transcription factor.

## INTRODUCTION

Metallochaperones are cytoplasmic proteins that traffic metal ions to other proteins including metalloenzymes and metal resistance systems (Carter *et al.*, 2009; Robinson & Winge, 2010). While most studies have focused on copper-metallochaperones, other metal specificities occur (Grossoehme *et al.*, 2007; Herbst *et al.*, 2010; Okamoto *et al.*, 2010). Much less is known about the trafficking of heavy metals such as mercury. In the case of proteobacteria, the mercury-specific transport protein, MerP, binds and transfers this metal to the integral membrane protein MerT, thereby depleting its concentration in the periplasmic space (Morby *et al.*, 1995; Serre *et al.*, 2004). Cytoplasmic trafficking of mercury has also been reported through transfer between cysteine residues encoded in the N-terminal domain of bacterial mercuric reductase (Hong *et al.*, 2010).

Microbes that inhabit naturally occurring metal-rich niches provide an opportunity to identify and study novel metal resistance mechanisms. The order *Sulfolobales* includes diverse thermoacidophilic microbes including species that inhabit hot metal-saturated locations (Orell *et al.*, 2010; Simbahan *et al.*, 2005; Wang *et al.*, 2011). Studies on mercury resistance in *Sulfolobus solfataricus* established the existence and critical regulatory features of an archaeal mercury resistance (*mer*) operon (Dixit *et al.*, 2004; Schelert *et al.*, 2004, 2006). The *S. solfataricus mer* locus encodes four genes where *merH*, *A* and *I* are arranged in one transcription unit and *merR* is divergently transcribed upstream of *merH*. Protein phylogenetic analysis and gene disruption studies indicated that *merA* encoded a mercuric reductase required for reduction of mercuric ion, Hg(II), to its elemental form, Hg(0) (Schelert *et al.*, 2004), despite its lack of an active tyrosine residue (Simbahan *et al.*, 2005) in its putative active site. *merI* (122 aa) is located 3′ to *merA* and is separated by a 142 nt intergenic region. It is expressed by constitutive transcription (from its own promoter, *merIp*) and by read-through transcription initiating upstream at *merHp*. Gene disruption studies, however, exclude a role for MerI in mercury resistance or *mer* regulation (Schelert *et al.*, 2006). The *S. solfataricus* MerR transcription factor regulates *merHAI* transcription in a metal-dependent fashion, and site-specific mutations in the DNA binding site of *merR* created *in vivo* positioned the binding site immediately 5′ of the predicted *merHp* TATA box (Schelert *et al.*, 2006). Electrophoretic mobility shift assay demonstrated that MerR/*merHp* DNA complex formation was template specific and dependent on the

†Present address: James.Schelert@bioenergy.abengoa.com

Abbreviations: ICP-MS, inductively coupled plasma-mass spectrometry; OLEPCR, overlap extension PCR; qRT-PCR, quantitative reverse transcription-PCR; RT-PCR, reverse transcription-PCR.

The GenBank/EMBL/DDBJ accession numbers for the mercury resistance operon (complete) and the MerH 60 aa protein sequences of *S. solfataricus* strain 98/2 are EF151956.1 and ABL96629.1, respectively.

presence of the binding site, but was insensitive to Hg(II) addition as well as site-specific binding site mutations that relieved *in vivo merHp* repression (Schelert *et al.*, 2006).

While the roles of MerA and MerR have been determined, the function of MerH was unknown. The *merH* gene was first identified because of its Cys-Xaa$_{19–22}$-Cys-Xaa$_3$-Cys or CxCxC motif together with its location immediately adjacent to mercuric reductase (MerA) that suggested a role in trafficking of mercury (Ettema *et al.*, 2003). However, *S. solfataricus* MerH lacks homology to well characterized bacterial mercury binding proteins, such as periplasmic MerP and the N-terminal domains found in some MerA proteins (Barkay *et al.*, 2003) (but lacking in *S. solfataricus*), or to a membrane transporter called MerH in *Mycobacterium marinum* (Schué *et al.*, 2009). The results presented here suggest that *S. solfataricus* MerH is a mercury trafficking protein.

## METHODS

**Archaeal strains and cultivation.** Archaeal strains and plasmids are indicated (Table 1). Primer sequences are available upon request. *S. solfataricus* strain 98/2 and its derivatives were grown at 80 °C with aeration in batch culture as described previously (Allen, 1959; Rolfsmeier & Blum, 1995; Worthington *et al.*, 2003b) at 80 °C in Allen's basal salts (Allen, 1959) as modified (Brock *et al.*, 1972) at pH 3.0. Liquid media were supplemented with 0.2 % (w/v) sucrose (SM), 0.2 % (w/v) lactose or 0.2 % (w/v) tryptone (RM) as carbon and energy sources. Growth was monitored at 540 nm using a Cary 50 spectrophotometer (Varian). When investigating the effect of mercuric ion, cells were treated with $HgCl_2$ (Sigma) from a freshly made 10 mM stock.

**Strain construction.** Strain construction procedures were as described previously (Maezato *et al.*, 2011; Sowers *et al.*, 2007) unless otherwise noted. DNA was electroporated into strain PBL2025 (Table 1) and its derivatives. Recombinants were enriched and individuals isolated, screened and processed as described (Maezato *et al.*, 2011; Sowers *et al.*, 2007). PCR, restriction analysis and DNA sequencing were used to genotype alleles. Overlap extension PCR (OLEPCR; Higuchi *et al.*, 1988) was used to create site-specific mutations and DNA fusions. The *merRp*$_{TATA}$ (PBL2044) and *merHp*$_{TATA}$ (PBL2042) mutants were constructed by targeted recombination and markerless exchange as described previously (Maezato *et al.*, 2011; Sowers *et al.*, 2007) with plasmids pBN1050 and pBN1049, respectively. PCR of the *merRp*$_{TATA}$ and *merHp*$_{TATA}$ fragments used primers merR-L-*Bam*HI-F and merH-L-*Bam*HI-R (Schelert *et al.*, 2006) followed by insertion at the *Bam*HI site of pBN1035. *Bsa*JI sites in the TATA boxes of the *merRp* and *merHp* fragment were created by OLEPCR with primers p22 and p23 (*merRp*) or p18 and p19 (*merHp*). The *merHp*$_{TATA}$/*merAp*$_{TATA}$ double mutant (PBL2052) was constructed by markerless exchange using plasmid pBN1056 using primers merR-L-*Bam*HI-F and merH-L-*Bam*HI-R (Schelert *et al.*, 2006). The *Bsa*JI site located in the *merAp* TATA box of the *merHp*$_{TATA}$/*merAp*$_{TATA}$ fragment was created by OLEPCR with primers p10 and p11 using plasmid pBN1049 as the template so as to include the *merHp*$_{TATA}$ mutation. Plasmid pBN1056 was constructed by insertion of a *Bam*HI digested PCR of a *merHp*$_{TATA}$/*merAp*$_{TATA}$ amplicon into the *Bam*HI site of pBN1035. The *merH*$_{TAG}$ mutant (PBL2054) was constructed by markerless exchange using plasmid pBN1058 and primers merR-L-*Bam*HI-F and merH-L-*Bam*HI-R (Schelert *et al.*, 2006). The *Spe*I site located in the *merH* ORF of the *merH*$_{TAG}$ fragment was created by OLEPCR with primers p16 and p17 using WT genomic DNA as the template. Plasmid pBN1058 was constructed by insertion of a *Bam*HI digested PCR of a *merH*$_{TAG}$ amplicon into the *Bam*HI site of pBN1035. The *merH* in-frame deletion mutant (PBL2114) was constructed by OLEPCR and markerless exchange as described previously (Schelert *et al.*, 2006) using pBN1035. Two different PCRs were used to generate fragments identical in sequence to either end of the *merH* region targeted for deletion using primer p31 combined with p29 and primer p31 combined with p32. These amplicons were annealed at their overlapping region and amplified using OLEPCR to produce a single amplicon. The *merH* in-frame deleted product was then cloned at the *sph*I site of pBN1035 and integrated by markerless exchange.

***merA* expression plasmids and archaeal hosts.** Construction of the *S. solfataricus* mercury-inducible *merA* expression strain (PBL2045) used markerless exchange (Schelert *et al.*, 2006) and plasmids pBN1052 and pBN1000. Primers p8 and p28 were used to amplify *merA* from WT cells followed by insertion into *Nhe*I/*Bam*HI sites of plasmid pET28B to make pBN1000. A hexahistadine tag was fused to the N terminus of *merA* and a 69 nt fragment was added 5′ to the *merA* start codon derived from pET28b. Primers p13 and merR-L-*Bam*HI-F (Schelert *et al.*, 2006) were used to amplify *merR* and flanking regions from strain PBL2000 to create a *merRH* fragment. OLEPCR was used to fuse and extend his$_6$-*merA* and *merRH* PCR amplicons. pBN1052 was made using primers p12 and merH-L-*Bam*HI-R to amplify the his$_6$-*merA* fragment from pBN1000 followed by digestion and insertion into the *Bam*HI site of pBN1035 (Schelert *et al.*, 2006). Construction of the *merR*$_{TATA}$ *merA* expression strain (PBL2048) used markerless exchange (Schelert *et al.*, 2006) and plasmid pBN1053. Primers merR-L-*Bam*HI-F and merHp-L-*Bam*HI-R (Schelert *et al.*, 2006) were used to amplify the *merR*$_{TATA}$::*merA* expression fragment. The *Bsa*JI site located in the *merR* TATA box of the *merR*$_{TATA}$::*merA* expression fragment was created by OLEPCR with primers p18 and p19 and DNA from strain PBL2045 as template so as to include the N-terminal hexahistidine tag and thrombin site with *merA*. Plasmid pBN1053 was constructed by insertion of the *merR*$_{TATA}$::*merA* fragment into the *Bam*HI site of pBN1035 (Schelert *et al.*, 2006). Construction of the *merR*::*lacS merA* expression strain (PBL2053) used linear DNA transformation as described previously (Schelert *et al.*, 2006). Primers merR-L-*Bam*HI-F (Schelert *et al.*, 2006) and p13 were used to amplify the *merR*::*lacS*::*merA* fragment using plasmid pBN986 (Schelert *et al.*, 2004) as template.

**Single copy complementation analysis.** The *S. solfataricus* 98/2 pNOB8-like plasmid, designated here as p98-2, was isolated from mid-exponential phase WT (PBL2000) cells grown in RM using alkaline lysis extraction (Greve *et al.*, 2004). *Eco*RI-digested DNA was randomly cloned into pNEB193 and one of the resulting plasmids, pBNClone3, contained a fragment of a *trbE* conjugal transfer protein homologue (222/422 aa, 52 % identity to *trbE* from '*Sulfolobus islandicus*'). *trbE* was amplified from plasmid pBNClone3 using primers p1 and p3 and inserted at the *Eco*RI site of pNEB193 to form pBN1030 while the *trbE Bsp*EI site was created by OLEPCR with primers p2 and p4. An *S. solfataricus* strain 98/2 genomic BAC library (Amplicon Express) was constructed following *Eco*RI, *Bam*HI or *Hin*dIII digestion in agarose plugs followed by size fractionation by pulse field electrophoresis into the copy control plasmid pCC1BAC (Epicentre). Restriction analysis of representative isolates verified a mean insert size of approximately 108 kb and the resulting 1536 plasmid clones constituted 30-fold coverage. Of 259 BAC clones screened by colony PCR, three *trbE* containing BACs were found. BAC inserts from pBNSSC004E8, pBNSSC006D3 and pBNSSC007C4 were sequenced using primers p24 and p25 and localized the p98-2 plasmid to a 70 kb region spanning *S. solfataricus* ORFs SSO0451 (39 1180 nt) and SSO0583 (46 1484 nt). A 14 nt *S. solfataricus* plasmid integration site (Greve *et al.*, 2004) was identified within this region between ORFs SSO0507 and SSO0508. The identity of

**Table 1.** Microbial strains and plasmids

| Strain or plasmid | Genotype or sequence | Source or derivation |
|---|---|---|
| **Strain** | | |
| PBL2000 | WT *S. solfataricus* strain 98/2 | Lab collection |
| PBL2025 | *del*(*SSO3004-3050*) | PBL2000 (Schelert *et al.*, 2004) |
| PBL2042 | *merH-TATA-BsaJI* | PBL2025 by markerless exchange |
| PBL2044 | *merR-TATA-BsaJI* | PBL2025 by markerless exchange |
| PBL2045 | *merA-N-His* | PBL2025 by markerless exchange |
| PBL2048 | *merR-TATA-BsaJI/merA-N-His* | PBL2025 by markerless exchange |
| PBL2052 | *merH-TATA-BsaJI/merA-TATA-BsaJI* | PBL2042 by markerless exchange |
| PBL2053 | *merR*::*lacS/merA-N-His* | PBL2025 by linear recombination |
| PBL2055 | *merH-TAG-SpeI* | PBL2025 by markerless exchange |
| PBL2060 | *merH-TAG-SpeI/trbE*::*merHA*::*lacS* | PBL2054 by linear recombination |
| PBL2114 | *merH* in-frame deletion by OLEPCR *(SphI)* | PBL2025 by markerless exchange |
| **Plasmid** | | |
| pCC1BAC | *Bla* | Amplicon Express; this work |
| pNEB193 | *Bla* | NE Biolabs |
| pBN1000 | *merA-N-His (NheI-BamHI)* | pBN990; this work |
| pBN1030 | *trbE (EcoRI)* | pNEB193, NE Biolabs; this work |
| pBN1033 | *trbE*::*merHA (BspeI)* | pBN1030; this work |
| pBN1035 | *lacS (KpnI)* | pUC19 (Schelert *et al.*, 2006) |
| pBN1049 | *lacS (KpnI), merH-TATA-BsaJI (BamHI)* | pBN1035; this work |
| pBN1050 | *lacS (KpnI), merR-TATA-BsaJI (BamHI)* | pBN1035; this work |
| pBN1052 | *lacS (KpnI), merA-N-His(NheI-BamHI)* | pBN1035; this work |
| pBN1053 | *lacS (KpnI), merR-TATA-BsaJI*::*merA-N-His(NheI-BamHI)* | pBN1035; this work |
| pBN1056 | *lacS (KpnI), merH-TATA-BsaJI/merA-TATA-BsaJI* | pBN1035; this work |
| pBN1058 | *lacS (KpnI), merH-TAG-SpeI* | pBN1035; this work |
| pBN1061 | *trbE*::*merHA*::*lacS (MfeI)* | pBN1033; this work |
| pBN986 | *merR*::*lacS* | pUC19 (Schelert *et al.*, 2004) |
| pET28b | *Kan* | Novagen |
| pBNClone3 | *trbE (EcoRI)* | pNEB193; this work |
| p98-2 | *S. solfataricus* 98-2 plasmid isolated from PBL2000 | This work |
| pBNSSC004E8 | *trbE* | pCC1BAC, Amplicon Express; this work |
| pBNSSC006D3 | *trbE* | pCC1BAC, Amplicon Express; this work |
| pBNSSC007C4 | *trbE* | pCC1BAC, Amplicon Express; this work |

genes flanking *trbE* was determined by BAC DNA sequencing using primers p27 and p26. Genes flanking *trbE* were identified as *traC* (30/98 aa, 30 % identity to *traC* from '*Sulfolobus tengchongensis*' plasmid pTC) and pTC_p16 (28/74 aa, 37 % identity to pTC_p16 from '*S. tengchongensis*' plasmid pTC). Construction of the $merH_{TAG}/merH_{REP}$ mutant (PBL2060) employed transformation by targeted recombination (Schelert *et al.*, 2006) using plasmid pBN1061 and strain PBL2054 using primers p20 and p21. Plasmid pBN1033 was constructed by insertion of a *Bsp*EI-digested *merHA* amplicon into the *Bsp*EI site of *trbE* in plasmid pBN1030. Plasmid pBN1061 was constructed by insertion of a *lacS* amplicon into the naturally occurring *Mfe*I site in *merA* (Schelert *et al.*, 2004) in plasmid pBN1033 using primers lacS-*Mfe*I-F and lacS-*Mfe*I-R (Schelert *et al.*, 2004).

**Reverse transcription-PCR.** Quantitative reverse transcription-PCR (qRT-PCR) using SYBR-I Green and a real-time PCR instrument (Eppendorf Mastercycler) was performed as described by the manufacturer or, as described by Bradford *et al.* (2005), using a variable range of PCR cycles (Marone *et al.*, 2001; Nakayama *et al.*, 1992) with RNA prepared according to described methods (Bini *et al.*, 2002; Haseltine *et al.*, 1999a). The exponential range of PCR product abundance (Noonan *et al.*, 1990) was determined for all targets and product qualities were verified by examination of melting curves. Parallel RT-PCR amplifications were used to evaluate RNA levels from experimental genes relative to those of the reference gene, *tbp*, or 7S rRNA, as described (Lesur & Campbell, 2004; Schelert *et al.*, 2006). RNA was treated to remove DNA by addition of 1 U DNase I (Fermentas) per μg of total RNA at room temperature for 15 min and then neutralized with 2 μl 25 mM EDTA and incubated at 70 °C for 10 min. cDNA synthesis used 20 pmoles of PCR antisense primer, 20 mM dNTPs mix (Invitrogen) and 200 U M-MuLV reverse transcriptase (Fermentas), for 60 min at 37 °C. Synthesized cDNA was subjected to standard PCR and analysed using 2 % (w/v) TBE agarose gels. Initial semi-quantitative reverse transcription-PCR (RT-PCR) was performed according to a cDNA amplification protocol (Sambrook & Russell, 2001) using a variable range of PCR cycles (Bradford *et al.*, 2005; Marone *et al.*, 2001; Nakayama *et al.*, 1992) with RNA prepared as described (Bini *et al.*, 2002; Haseltine *et al.*, 1999b) and treated to remove DNA by addition of 1U DNase I (Fermentas) per μg of total RNA at room temperature for 15 min. RNA was denatured by adding 25 mM EDTA and heating for 10 min at 70 °C. cDNA synthesis was primed using 20 pmoles RT-PCR primers p14 (*merH*), p7 (*merA*) and p5 (7S RNA), 20 mM dNTPs mix (Fermentas) and 200 U M-MuLV reverse transcriptase (Fermentas), for 60 min at 37 °C followed by standard PCR using primers p15 and p14 (*merH*), p9 and p7 (*merA*), and p6 and p5 (7S RNA) and monitored using 2 % TBE agarose gels.

**Identification, purification and characterization of MerA.** For detection of MerA in whole-cell extracts, samples were recovered from cultures that had been treated with mercuric chloride (0.3 μM) at a cell density of $10^8$ ml$^{-1}$ (0.1 $OD_{540}$) and harvested 4 h later. Cell suspensions were prepared using intermittent sonication then analysed by 2D SDS-PAGE as described by Hajduch *et al.* (2005). Spots were sequenced by tandem mass spectrometry (MS/MS) and peptides identified by local BLAST against the *S. solfataricus* proteome. His-tagged recombinant MerA protein was isolated from the *S. solfataricus mer*-inducible expression strain PBL2045 and the *mer* constitutive expression strains PBL2048 and PBL2053. MerA synthesis in PBL2045 was induced by mercuric chloride treatment (0.3 μM) in 500 ml cultures with additional incubation (4 h). Use of PBL2048 and PBL2053 obviated metal treatment and cells could be grown in larger scale (10 l) as described (Schelert *et al.*, 2004; Worthington *et al.*, 2003a) or using 3 l Aplikon bioreactors at 80 °C, pH 3.0, with mixing (200 r.p.m.) and aeration (1 volume of air per volume of medium per min). Cell pellets were stored at −20 °C or resuspended in 10 ml buffer A (50 mM Tris/HCl pH 7.8, 0.5 M NaCl, 10 % glycerol and 20 mM β-mercaptoethanol) and then lysed using pulsed sonication or pressure (French pressure cell with passage twice at 12 000 p.s.i.). Lysates were clarified by centrifugation for 10 min (5000 ***g***) then processed by repeated nickel-affinity chromatography as described (Novagen). Protein eluted using 0.5 M imidazole was dialysed into buffer B pH 7.0 (100 mM Tris pH 9.0, 1 mM β-mercaptoethanol). Samples analysed by SDS-PAGE used either 12.5 or 16 % polyacrylamide gels. Protein concentrations were determined by BCA assay (Pierce). MerA protein yields were 2.0 mg l$^{-1}$ of culture, equivalent to 2.5 % of total protein. Reductase assays were performed as described by Fox & Walsh (1982) using an Agilent Cary100 UV-Vis spectrophotometer at 65 °C in 100 mM Tris/HCl (pH 9.0) containing 100 μM β-mercaptoethanol, 200 μM NADPH and 100 μM mercuric chloride. Reactions were initiated by NADPH addition and mercury-dependent oxidation of NADPH was monitored by the rate of decrease in absorbance at 340 nm. Control reactions were performed without enzyme and without metal addition and the difference in slopes was subtracted from reactions containing all components. FAD (100 μM) was added to reaction mixtures to monitor its effect on enzymic activity. Efforts to reactivate MerA thiol groups involved sample dialysis into tris(3-hydroxypropyl)phosphine (0.5 mM) followed by enzyme assay. Specific activity was recorded in units (U) representing μmol NADPH oxidized min$^{-1}$ (mg protein)$^{-1}$ (Fox & Walsh, 1982). MerA absorbance spectra were examined at a protein concentration of 5 mg ml$^{-1}$ using an Agilent Cary100 UV-Vis spectrophotometer at room temperature.

**Mercury resistance determination.** Strains were grown with aeration in a defined minimal medium (SM). At a cell density of $10^8$ cells ml$^{-1}$, 0.5 μM mercuric chloride unless otherwise indicated was added to each culture. Cultures of strains with no added mercury were included as controls. Growth was monitored by measuring the absorbance at 540 nm and growth curves were plotted. All cultivation experiments were repeated at least three times and representative data are shown from these biological repeats.

**Molecular biology methods.** DNA cloning, PCR and plasmid transformation of *Escherichia coli* were performed as described (Haseltine *et al.*, 1999c; Rockabrand *et al.*, 1998). DNA sequencing was as described by Rolfsmeier *et al.* (1998). DNA and RNA concentrations were measured using either a DyNA Quant 200 fluorometer (Hoefer) or a UV–visible spectrophotometer Genesys 2 (Spectronics). All manipulations of RNA were as described (Bini *et al.*, 2002; Haseltine *et al.*, 1999b). Protein concentrations were measured using the BCA Protein Assay Reagent kit (Pierce). Unless otherwise indicated, all chemicals were obtained from common chemical suppliers.

**Inductively coupled plasma-MS analysis.** To determine the intracellular concentrations of mercury, cells were grown to an optical density (540 nm) of 0.1, corresponding to approximately $10^8$ cells ml$^{-1}$ and treated with 0.5 μM mercuric chloride from a freshly made 10 mM stock. Samples (1 ml) were then removed at the indicated time points and cells were harvested by centrifugation at 10 000 ***g*** for 5 min followed by two successive washes using distilled water to remove free mercury. Cell pellets were frozen at −20 °C for subsequent analysis. Cell pellets were extracted using 50 μl concentrated nitric acid and the resulting extracts analysed by inductively coupled plasma-mass spectrometry (ICP-MS) using an Agilent ICP-MS 7500cx. A certified mercury reference standard was used for sample normalization. All values are the means of samples from replicate cultures.

## RESULTS

### Effect of a *merH* nonsense mutation

To assess the role of MerH in metal detoxification, a premature stop codon was created in the *merH* gene of the WT strain (Fig. 1a, c). The $merH_{TAG}$ mutant (PBL2054) was created by transforming strain PBL2025 with plasmid pBN1058 using markerless exchange as described (Schelert *et al.*, 2006). To assess the physiological consequence of the $merH_{TAG}$ mutation, the response of the mutant strain to mercuric chloride challenge was compared to that of the otherwise isogenic WT strain and a *merA* mutant (Fig. 2a). When treated with mercury, growth of the $merH_{TAG}$ mutant was strongly inhibited by metal addition relative to the WT strain and nearly identical to the pattern exhibited by the *merA* mutant.

### Single copy *merH* complementation analysis

To determine the importance of MerH in the $merH_{TAG}$ mutant's sensitivity to mercury, a functional copy of *merH* under the control of its native promoter (*merHp*) was reintroduced as a single copy chromosomal insertion (Fig. 1b). The inserted DNA encoded both WT *merH*, an inactivated copy of *merA* disrupted by *lacS* thereby providing a selection for DNA integration, and flanking DNA sequences to target integration. Recombinants were obtained by linear DNA recombination as described (Maezato *et al.*, 2011; Schelert *et al.*, 2006) using the $merH_{TAG}$ mutant as the host. The site of insertion was within the *trbE* gene of an integrated copy of plasmid p98-2 (Greve *et al.*, 2004) present in the chromosome of *S. solfataricus* strain 98/2. The *trbE* gene was used because the plasmid genes were unlikely to be involved in metal resistance. As the second copy of *merH* was inserted within an integrated conjugative pNOB8-like plasmid named p98-2, plasmid segregation was evaluated by enumerating loss of *lacS* located in the flanking *merA* region. Segregation within the metal-treated population was not detectable (<0.1 %). The response of the *merH*-complemented strain to mercuric chloride (0.5 μM) challenge was compared to that of the otherwise isogenic WT and parental strain during growth in SM (Fig. 2b). The merodiploid strain

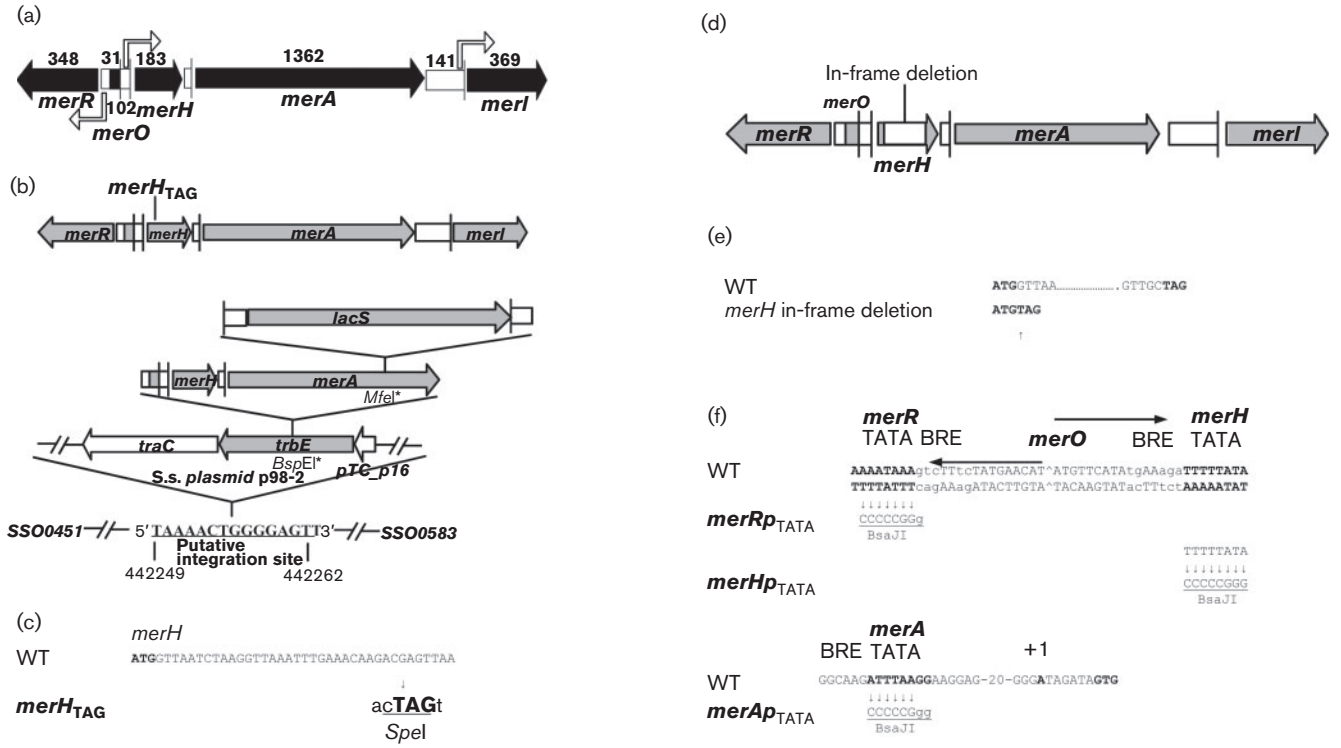


**Fig. 1.** Introduction to the mutations in the *mer* operon. (a) Schematic of the *mer* operon. Solid arrows indicate transcribed ORFs and open rectangles indicate intergenic regions. Nucleotide lengths are indicated. Promoters are indicated by right angle arrows. (b) Schematic of the complemented $merH_{TAG}$ mutant by single copy $merH^{+}$ integration. Location of the $merH_{TAG}$ point mutation in the *merH* locus (top). Reintroduction of WT *merH* at the *trbE* locus (bottom); the *merA* gene is disrupted by *lacS*. (c) DNA sequence of the $merH_{TAG}$ mutation and addition of new diagnostic restriction site. (d) Schematic of the *merH* in-frame deletion mutant. Location of the in-frame deletion in the *merH* locus is indicated by an open box. (e) DNA sequence of the *merH* in-frame deletion mutation including retention of start and stop codons. (f) DNA sequences of *mer* promoter mutations for $merHp_{TATA}$, $merRp_{TATA}$ and $merAp_{TATA}$.

remained significantly more sensitive to metal challenge than the WT strain but more resistant than the $merH_{TAG}$ mutant. This result indicated that MerH complementation could reconstitute at least partial mercury resistance but the contribution of translational polarity on downstream expression of *merA* remained unclear.

## Polycistron and promoter analysis

More precise mutant analysis was necessary to determine the *in vivo* contributions of MerH and MerA on the phenotype of the $merH_{TAG}$ mutant. Though previous studies had provided information on the *mer* regulatory region including the MerR binding site and the *merH* transcription start site (Schelert *et al.*, 2006), the location of the *mer* operon promoter(s) had not been determined. As proposed previously, occurrence of a putative promoter located immediately 5′ of *merA* (Schelert *et al.*, 2004) would circumvent a requirement for *merHA* cotranscription and therefore change the identity of the *mer* polycistron. To clarify the identity of the primary *mer* promoter, the predicted sequences were modified by markerless exchange and the resulting mutants characterized. Mutant strains ($merR_{TATA}$ and $merH_{TATA}$) were created in which the T/A-rich octameric sequences centred 26 nt upstream of the *merR* or *merH* (Schelert *et al.*, 2006) transcription start site, or 33 nt upstream of the *merA* transcription start ($merA_{TATA}$) (Schelert *et al.*, 2004), were replaced with G/C-rich sequences and the insertion of a *Bsa*JI site (Fig. 1f). To assess the physiological consequence of the mutations, the response to mercuric chloride challenge was evaluated relative to controls during growth in defined medium (SM). Higher metal doses were used to accentuate strain differences. While the $merHp_{TATA}$ mutant was more sensitive than the WT to metal challenge, it retained significant resistance relative to the *merA* disruption mutant (Fig. 2d). Because there was a lag associated with the growth of the $merHp_{TATA}$ mutant compared to the WT, the TATA box mutation may have negatively affected *merHp* activity resulting in a reduction or delay in *merHA* transcript production. Residual resistance of the $merHp_{TATA}$ mutant might arise from the activity of an internal promoter located upstream of *merA* (Schelert *et al.*, 2004). This was tested by insertion of a G/C-rich mutation

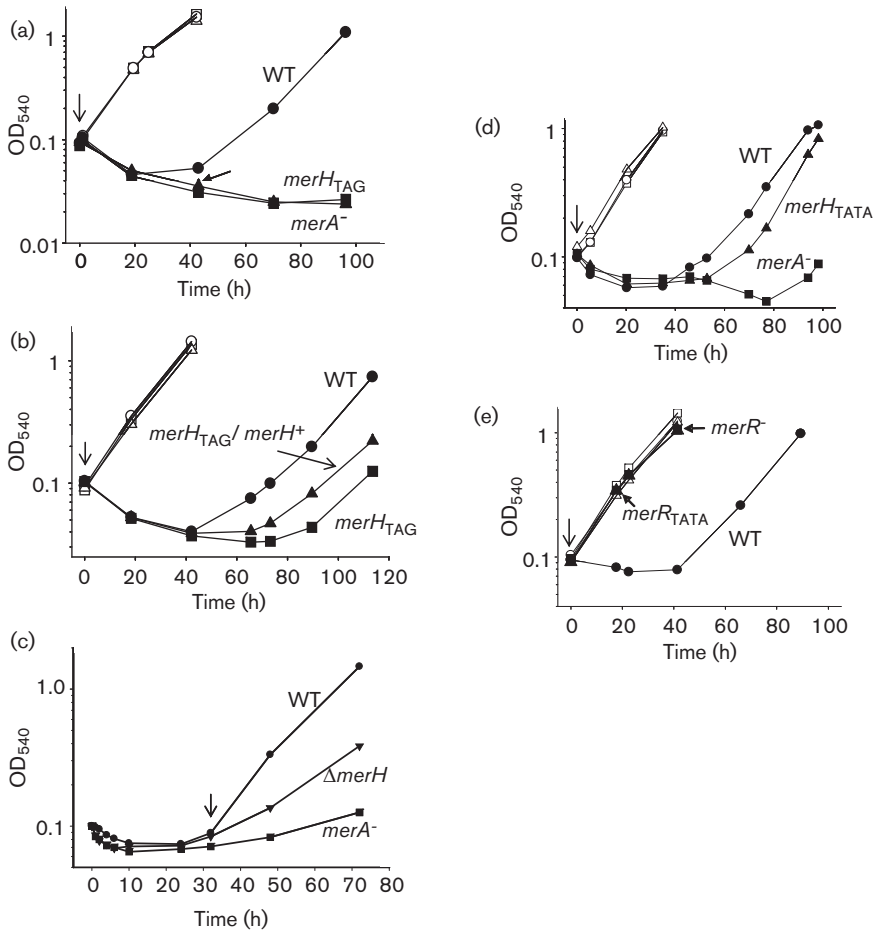


**Fig. 2.** Response of *mer* operon mutants to mercuric chloride. All strains were treated with mercuric chloride (arrows) at 0.5 μM unless otherwise indicated. Closed symbols (treated cultures), open symbols (untreated cultures). (a) $merH_{TAG}$ mutant (squares), *merA* mutant (triangles) or WT (circles). (b) $merH_{TAG}$ (triangles), $merH_{TAG}$/$merH^+$ (squares) and WT (circles). (c) Δ*merH* in-frame deletion mutant (inverted triangles), *merA* mutant (squares) and WT (circles). RNA was extracted for qRT-PCR analysis of *merA* at 32 h post-challenge (arrow). (d) $merHp_{TATA}$ mutant (triangles), *merA* disruption mutant (squares) and WT (circles) treated with 0.75 μM mercuric chloride. (e) $merRp_{TATA}$ mutant (squares), *merR* mutant (triangles) or WT (circles). Cultivation experiments were repeated at least three times.

centred 33 nt from the *merA* transcription start site in the $merHp_{TATA}$ mutant background creating a double mutation (Fig. 1f). The double TATA box mutant had identical sensitivity towards metal challenge relative to its parent ($merH_{TATA}$) indicating that the proposed *merA* promoter was not functional. In contrast, the $merRp_{TATA}$ mutant was more resistant to metal challenge than the WT and similar to the *merR* disruption mutant (Fig. 2e). Similarity between the phenotype of the $merRp_{TATA}$ mutant and the *merR* disruption mutant suggested that there was constitutive expression of the *mer* operon in this strain due to loss of MerR production.

## MerH in-frame deletion

To further understand the contribution of MerH towards mercury resistance, an in-frame *merH* deletion mutant containing both *merH* start and stop codons was constructed (Fig. 1d, e). This strain avoided the complication of polarity inherent to the system described above using the *merH*-complemented $merH_{TAG}$ mutant. Like the *merH* merodiploid, the in-frame *merH* deletion mutant was more resistant to Hg(II) than a *merA* mutant but more sensitive than the WT (Fig. 2c).

## *S. solfataricus*-derived MerA protein purification and analysis

Despite reduction of MerA levels observed in $merH_{TAG}$ mutant extracts (Fig. 3c), it remained possible that MerH was catalytically required for MerA activity and metal resistance was therefore compromised in the mutant strain. To determine whether or not MerA alone could reduce Hg(II) to Hg(0), it was necessary to obtain purified MerA

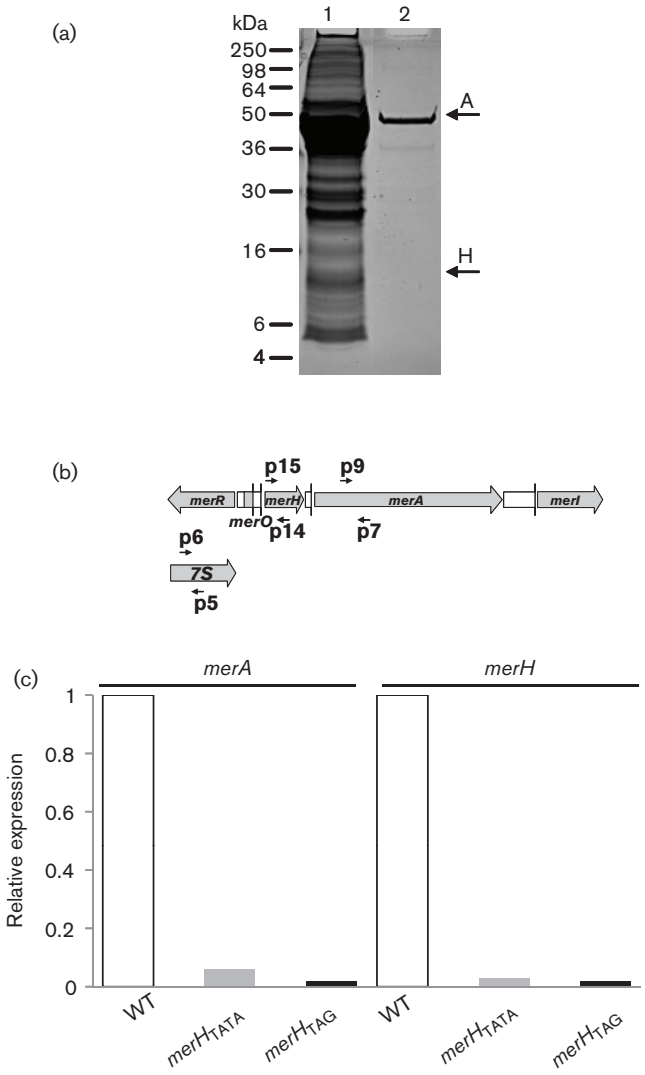


**Fig. 3.** MerA protein purification and effect of *merH* mutations on *mer* transcript abundance. (a) Expression and purification of polyhistidine-tagged MerA from an *S. solfataricus* MerA expression strain. Ni-NTA purified samples were analysed by 1D SDS-PAGE on a 12.5 % acrylamide gel. Lanes: 1, single passaged Ni-NTA eluant; 2, double passaged Ni-NTA eluant (3.6 μg protein loaded). (b) qRT-PCR primer locations. (c) qRT-PCR analysis of *merH* and *merA* mRNA. *merH* and *merA* transcript abundance normalized to 7S RNA were determined in total RNA 4 h after challenge with 0.3 μM Hg(II) from the WT, $merHp_{TATA}$ and $merH_{TAG}$ strains. Technical repeats produced less than 10 % variation between results.

protein. Attempts to produce MerA in *E. coli* were not successful, therefore the protein was overproduced instead in *S. solfataricus* using a mercury-inducible expression construct with the *merHp* promoter integrated into the chromosome. A hexahistidine tag was positioned at the N terminus of MerA because cysteine residues located at the C-terminal end of MerA form part of the active site in the MerA homodimer and a tag at this end may have interfered with MerA enzymic activity. To assess the physiological effect of the N-terminal hexahistidine tag on MerA activity *in vivo*, the response of the MerA expression mutant strain (PBL2045) to mercuric chloride challenge was compared to that of the otherwise isogenic WT strain and the *merA* disruption mutant. The three strains were grown in defined medium and at a cell density of $10^8$ cells $ml^{-1}$, 0.3 μM mercuric chloride was added to each culture. Cultures of all strains with no added mercury were included as controls. Growth of the *S. solfataricus* MerA expression mutant was similar to the WT strain indicating that the N-terminal hexahistidine tagged MerA was active *in vivo*. The *merA* disruption mutant was included as a control and exhibited a significantly longer lag than WT. Mercury induction of the MerA expression mutant resulted in production of MerA (49 kDa) in sufficient abundance to be detected by Coomassie blue staining following 2D SDS-PAGE (data not shown), and one more purification by nickel-affinity chromatography (Fig. 3a). Protein sequencing by MS/MS confirmed the identity of the protein as *S. solfataricus* MerA. An alternative strain, PBL2048, was then constructed in which *merA* was expressed constitutively by blocking MerR synthesis due to TATA box inactivation of *merRp*. To assess the physiological effect of the hexahistidine tag and to verify that MerA remained active, the response of strain PBL2048 was evaluated by metal treatment relative to the WT. The absence of a growth lag for PBL2048 despite metal addition demonstrated that MerA was active and constitutively produced. Purified protein (Fig. 3a, lane 2) had a specific activity of 0.30 U $mg^{-1}$ ($\pm$0.02) for mercury-dependent NADPH oxidation. Spectroscopic analysis of purified protein did not indicate presence of FAD-associated absorption peaks (340, 450) at protein concentrations of 5 mg $ml^{-1}$, while FAD addition (100 μM) had no impact on enzyme activity. Thiol reactivation by dialysis of MerA using tris(3-hydroxypropyl)phosphine also did not affect MerA activity. Since MerH protein was not evident in the purified active MerA protein samples, MerH was not required for MerA catalysis *in vitro*.

## Effect of *merH* mutations on *merH* and *merA* expression

qRT-PCR analysis was used to determine the impact of the $merHp_{TATA}$ mutation on transcript abundance and to determine if the $merH_{TAG}$ mutation influenced *merA* transcript abundance (Fig. 3b, c). Parallel qRT-PCR amplifications were used to evaluate RNA levels from experimental genes relative to those of the 7S rRNA reference gene as described previously (Lesur & Campbell, 2004; Schelert *et al.*, 2006). Batch cultures grown in defined medium were treated with 0.3 μM mercuric chloride, and samples were removed for analysis at times thereafter. The lower dose of mercuric chloride was used for these experiments because this dose was sufficient to induce expression of the *merHA* transcript without significantly retarding cell growth. Prior to mercury addition (0 h),

*merH* and *merA* RT-PCR products were not detected in the WT, $merHp_{TATA}$ or $merH_{TAG}$ mutants (data not shown). After mercury addition (4 h), *merH* and *merA* RT-PCR products were detected in all strains yet their abundance was significantly reduced in both the $merH_{TATA}$ mutant and the $merH_{TAG}$ mutant relative to the WT (Fig. 3c). MerA protein abundance in the $merH_{TAG}$ mutant was also evaluated using 2D SDS-PAGE and extracts from previously constructed *merR* and *merA* disruption mutants (Schelert *et al.*, 2004; data not shown). MerA protein abundance was significantly reduced in the $merH_{TAG}$ mutant and likely the cause of the $merH_{TAG}$ mutant phenotype of reduced metal resistance.

### Intracellular concentrations of mercury

To understand the specific contribution of MerH towards metal resistance, ICP-MS of whole-cell extracts was used to measure intracellular levels of mercury in the WT, *merH* deletion and *merA* mutant strains during metal challenge. In the WT strain, intracellular mercury underwent a rapid but transient increase within 5 h of metal challenge, returning to baseline 70 h later and commensurate with resumption of exponential growth (Fig. 4). In the mutants, a similar initial increase in mercury was observed, but both the amount of metal and its rate of return to pre-challenge levels were significantly different as compared to the WT strain. Both mutants accumulated higher levels of metal than the WT. In the case of the *merA* mutant this was consistent with loss of enzymic mercury reduction. Assuming MerA levels were unaffected by polarity in the *merH* deletion mutant, these results also indicated that MerH plays an important role in mediating metal resistance *in vivo*. Interestingly, the post-challenge rate of reduction of cell-associated mercury was slower for the *merH* deletion mutant than the *merA* mutant. In an attempt to distinguish between an effect of MerH deficicency on MerA reductase activity versus an effect on derepression of *merHA* transcription, qRT-PCR analysis was conducted of *merA* transcript abundance in the WT and *merH* deletion mutant during metal challenge. Samples were removed at a time (32 h post-challenge; Fig. 4a, arrow) when both *merH* deletion mutant phenotypes (increased mercury content and reduced growth rate) were apparent. At this time, the abundance of *merA* mRNA was 5-fold lower in the *merH* mutant relative to the WT after internal normalization to transcription factor B (*tfb*) mRNA levels (Fig. 4b). Thus, MerH deficiency reduced the rate of derepression of *merHA* in response to metal challenge leading to elevated metal content and slow growth. As *merHA* transcription requires that MerR bind mercury to enable its dissociation from *merHp* DNA (Schelert *et al.*, 2006), these data suggest that MerH promotes the interaction between MerR and mercury as part of the normal metal regulatory response. These data clarify the identity of the *merHA* operon and its promoter, showing that the $merH_{TAG}$ mutation was polar on the expression of *mer*A and, therefore, that both MerH and MerA deficiency could underlie mercuric ion mutant sensitivities.

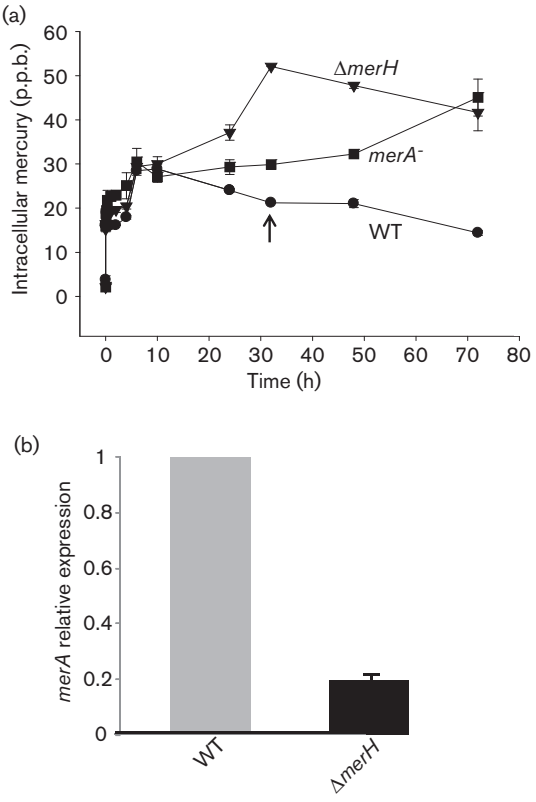


**Fig. 4.** Intracellular Hg measurement by ICP-MS analysis. (a) ICP-MS analysis of cell-associated mercury in parts per billion (p.p.b.). WT (closed circles), *merH* deletion mutant (inverted triangles) and *merA* disruption mutant (closed squares). (b) RNA was isolated from the Δ*merH* mutant and WT 32 h after 0.5 μM Hg(II) challenge and the relative *merA* transcript abundance was determined after normalization to *tbp* mRNA. Technical repeats produced less than 10 % variation between results.

## DISCUSSION

The data presented here indicate MerH as a likely mercury metallochaperone that plays a critical role mediating heavy metal resistance in the archaeon *S. solfataricus*. MerH trafficking of Hg(II) may have two distinct roles. By analogy to the actions of bacterial MerP (Gambill & Summers, 1992; Morby *et al.*, 1995; Serre *et al.*, 2004) and the N-terminal bacterial MerA motif (Hong *et al.*, 2010; Ledwidge *et al.*, 2005), archaeal MerH could facilitate metal transfer to MerA for reduction followed by metal efflux in its volatile state. However, as described here, MerH can also control derepression of transcription at the *merHp* promoter indicating its role in trafficking mercury to the MerR transcription factor. Transcription factor interactions of a metal chaperone offer new ways in which these proteins can control metal resistance mechanisms.

Interestingly, MerH has no homology to other proteins outside of a C-terminal domain, called TRASH, suggested previously to be involved in metal sensing and trafficking (Ettema *et al.*, 2003). The constitutively expressed *S. solfataricus* CopR transcription factor (Villafane *et al.*, 2011) (also called CopT; Ettema *et al.*, 2006) also encodes a TRASH domain and modulates copper resistance. These findings implicate the TRASH domain in the metabolism of two distinct metals, copper and mercury. However, the determinants of this domain that confer metal specificity remain to be identified.

In the present study, two genetic approaches were taken to evaluate MerH function. A nonsense mutation located at the 5′ end of *merH* resulted in mercury sensitivity. This mutation had a polar effect on *merA* expression; therefore, reduced metal resistance could reflect deficiencies of both MerA and MerH. Consistent with this observation, the introduction of a second but functional single copy of *merH* into the *merH* nonsense mutant strain but at a separate chromosomal location conferred only partial levels of mercury resistance. This effect was likely because MerA abundance remained low due to continued nonsense polarity of the *merH* nonsense mutation on *merA* expression. A second approach was therefore employed that used an in-frame deletion of *merH* to avoid nonsense polarity. However, in this case the continued reduction in *merA* expression arose from inefficient *merHA* derepression and not by polarity. The combination of these two genetic approaches indicated that MerH is a required component of mercury resistance.

Analysis of the $merH_{TAG}$ mutant established that the nonsense mutation compromised metal resistance by reducing both MerA protein and *merA* transcript abundance. Since this polar effect on gene expression is mediated through an effect on transcription, it closely resembles the process of polarity in bacteria. However, the mechanism responsible for polarity in archaea is unclear since homologues of the bacterial termination factor, Rho, are not evident in the genome of *S. solfataricus* or other archaea (Santangelo & Reeve, 2006), and bacterial terminators are largely absent (Ermolaeva *et al.*, 2000; Unniraman *et al.*, 2002). While cotranscription can be inferred by detection of transcribed intergenic sequences using RT-PCR, in the case of *mer* an internal promoter had been proposed that could bypass a requirement for coupled gene expression (Schelert *et al.*, 2004). Thus, an alternative strategy was required and TATA box mutagenesis was used to identify the main *mer* operon promoter. *S. solfataricus* promoters studied *in vitro* are typically T/A-rich octameric sequences while weaker noncanonical promoters are G/C-rich (Bell *et al.*, 1999; Reeve, 2003; Reiter *et al.*, 1990). In the data presented here, *in vivo* replacement of both *merRp*-TATA and *merHp*-TATA with G/C-rich octameric sequences resulted in reduced promoter activity and noticeable physiological effects while similar manipulations had no effect on a putative *merAp*. Because the mercury resistance phenotype of the $merRp_{TATA}$ mutant was similar to the *merR* disruption mutant, MerR was not produced and cells were unable to maintain repression of the *mer* operon. This confirms the identity of the *merRp* TATA box.

Curiously, *merHp* was not fully inactivated despite complete TATA box substitution with a sequence that bears no similarity to canonical crenarchaeotal promoters. This was evident in the $merHp_{TATA}$ mutant since it retained significantly higher resistance to Hg(II) than the *merA* disruption mutant (Fig. 2d). This finding may suggest that *merHp* functions as a TATA-less promoter or another promoter located elsewhere in the region may provide this function. In eukaryotes TATA-less Pol II promoters employ other proteins, notably TAFs, to ensure positioning of TBP/TFIID, proper DNA topology (bending) and Pol II recruitment (Wright *et al.*, 2006). As the *S. solfataricus* MerR protein remains DNA-bound during metal ligand interaction and is positioned immediately adjacent to the TATA box (Schelert *et al.*, 2006), MerR may provide a TAF-like function to ensure proper TBP positioning and RNAP recruitment. MerR and other bacterial-like archaeal transcription factors could constitute the functional archaeal TAFs that are also not evident in the genomes of these prokaryotes.

## ACKNOWLEDGEMENTS

This research was supported by NIH (1R01GM090209), DOD (HDTRA1-09-0030) and NSF (MCB-0085216). We thank Zach Pane for assistance in strain construction and R. M. Kelly for comments on the manuscript.

## REFERENCES

**Allen, M. B. (1959).** Studies with *Cyanidium caldarium*, an anomalously pigmented chlorophyte. *Arch Mikrobiol* **32**, 270–277.

**Barkay, T., Miller, S. M. & Summers, A. O. (2003).** Bacterial mercury resistance from atoms to ecosystems. *FEMS Microbiol Rev* **27**, 355–384.

**Bell, S. D., Kosa, P. L., Sigler, P. B. & Jackson, S. P. (1999).** Orientation of the transcription preinitiation complex in archaea. *Proc Natl Acad Sci U S A* **96**, 13662–13667.

**Bini, E., Dikshit, V., Dirksen, K., Drozda, M. & Blum, P. (2002).** Stability of mRNA in the hyperthermophilic archaeon *Sulfolobus solfataricus*. *RNA* **8**, 1129–1136.

**Bradford, W. D., Cahoon, L., Freel, S. R., Hoopes, L. L. & Eckdahl, T. T. (2005).** An inexpensive gel electrophoresis-based polymerase chain reaction method for quantifying mRNA levels. *Cell Biol Educ* **4**, 157–168.

**Brock, T. D., Brock, K. M., Belly, R. T. & Weiss, R. L. (1972).** *Sulfolobus*: a new genus of sulfur-oxidizing bacteria living at low pH and high temperature. *Arch Mikrobiol* **84**, 54–68.

**Carter, E. L., Flugga, N., Boer, J. L., Mulrooney, S. B. & Hausinger, R. P. (2009).** Interplay of metal ions and urease. *Metallomics* **1**, 207–221.

**Dixit, V., Bini, E., Drozda, M. & Blum, P. (2004).** Mercury inactivates transcription and the generalized transcription factor TFB in the archaeon *Sulfolobus solfataricus*. *Antimicrob Agents Chemother* **48**, 1993–1999.

**Ermolaeva, M. D., Khalak, H. G., White, O., Smith, H. O. & Salzberg, S. L. (2000).** Prediction of transcription terminators in bacterial genomes. *J Mol Biol* **301**, 27–33.

**Ettema, T. J., Huynen, M. A., de Vos, W. M. & van der Oost, J. (2003).** TRASH: a novel metal-binding domain predicted to be involved in heavy-metal sensing, trafficking and resistance. *Trends Biochem Sci* **28**, 170–173.

**Ettema, T. J., Brinkman, A. B., Lamers, P. P., Kornet, N. G., de Vos, W. M. & van der Oost, J. (2006).** Molecular characterization of a conserved archaeal copper resistance (cop) gene cluster and its copper-responsive regulator in *Sulfolobus solfataricus* P2. *Microbiology* **152**, 1969–1979.

**Fox, B. & Walsh, C. T. (1982).** Mercuric reductase. Purification and characterization of a transposon-encoded flavoprotein containing an oxidation-reduction-active disulfide. *J Biol Chem* **257**, 2498–2503.

**Gambill, B. D. & Summers, A. O. (1992).** Synthesis and degradation of the mRNA of the Tn21 mer operon. *J Mol Biol* **225**, 251–259.

**Greve, B., Jensen, S., Brügger, K., Zillig, W. & Garrett, R. A. (2004).** Genomic comparison of archaeal conjugative plasmids from *Sulfolobus*. *Archaea* **1**, 231–239.

**Grossoehme, N. E., Mulrooney, S. B., Hausinger, R. P. & Wilcox, D. E. (2007).** Thermodynamics of $Ni^{2+}$, $Cu^{2+}$, and $Zn^{2+}$ binding to the urease metallochaperone UreE. *Biochemistry* **46**, 10506–10516.

**Hajduch, M., Ganapathy, A., Stein, J. W. & Thelen, J. J. (2005).** A systematic proteomic study of seed filling in soybean. Establishment of high-resolution two-dimensional reference maps, expression profiles, and an interactive proteome database. *Plant Physiol* **137**, 1397–1419.

**Haseltine, C., Montalvo-Rodriguez, R., Bini, E., Carl, A. & Blum, P. (1999a).** Coordinate transcriptional control in the hyperthermophilic archaeon *Sulfolobus solfataricus*. *J Bacteriol* **181**, 3920–3927.

**Haseltine, C., Montalvo-Rodriguez, R., Carl, A., Bini, E. & Blum, P. (1999b).** Extragenic pleiotropic mutations that repress glycosyl hydrolase expression in the hyperthermophilic archaeon *Sulfolobus solfataricus*. *Genetics* **152**, 1353–1361.

**Herbst, R. W., Perovic, I., Martin-Diaconescu, V., O'Brien, K., Chivers, P. T., Pochapsky, S. S., Pochapsky, T. C. & Maroney, M. J. (2010).** Communication between the zinc and nickel sites in dimeric HypA: metal recognition and pH sensing. *J Am Chem Soc* **132**, 10338–10351.

**Higuchi, R., Krummel, B. & Saiki, R. K. (1988).** A general method of *in vitro* preparation and specific mutagenesis of DNA fragments: study of protein and DNA interactions. *Nucleic Acids Res* **16**, 7351–7367.

**Hong, B., Nauss, R., Harwood, I. M. & Miller, S. M. (2010).** Direct measurement of mercury(II) removal from organomercurial lyase (MerB) by tryptophan fluorescence: NmerA domain of coevolved $\gamma$-proteobacterial mercuric ion reductase (MerA) is more efficient than MerA catalytic core or glutathione. *Biochemistry* **49**, 8187–8196.

**Ledwidge, R., Patel, B., Dong, A., Fiedler, D., Falkowski, M., Zelikova, J., Summers, A. O., Pai, E. F. & Miller, S. M. (2005).** NmerA, the metal binding domain of mercuric ion reductase, removes $Hg^{2+}$ from proteins, delivers it to the catalytic core, and protects cells under glutathione-depleted conditions. *Biochemistry* **44**, 11402–11416.

**Lesur, I. & Campbell, J. L. (2004).** The transcriptome of prematurely aging yeast cells is similar to that of telomerase-deficient cells. *Mol Biol Cell* **15**, 1297–1312.

**Maezato, Y., Dana, K. & Blum, P. (2011).** Engineering thermo-acidophilic archaea using linear DNA recombination. *Methods Mol Biol* **765**, 435–445.

**Marone, M., Mozzetti, S., De Ritis, D., Pierelli, L. & Scambia, G. (2001).** Semiquantitative RT-PCR analysis to assess the expression levels of multiple transcripts from the same sample. *Biol Proced Online* **3**, 19–25.

**Morby, A. P., Hobman, J. L. & Brown, N. L. (1995).** The role of cysteine residues in the transport of mercuric ions by the Tn501 MerT and MerP mercury-resistance proteins. *Mol Microbiol* **17**, 25–35.

**Nakayama, H., Yokoi, H. & Fujita, J. (1992).** Quantification of mRNA by non-radioactive RT-PCR and CCD imaging system. *Nucleic Acids Res* **20**, 4939.

**Noonan, K. E., Beck, C., Holzmayer, T. A., Chin, J. E., Wunder, J. S., Andrulis, I. L., Gazdar, A. F., Willman, C. L., Griffith, B. & Von Hoff, D. D. (1990).** Quantitative analysis of MDR1 (multidrug resistance) gene expression in human tumors by polymerase chain reaction. *Proc Natl Acad Sci U S A* **87**, 7160–7164.

**Okamoto, S., Van Petegem, F., Patrauchan, M. A. & Eltis, L. D. (2010).** AnhE, a metallochaperone involved in the maturation of a cobalt-dependent nitrile hydratase. *J Biol Chem* **285**, 25126–25133.

**Orell, A., Navarro, C. A., Arancibia, R., Mobarec, J. C. & Jerez, C. A. (2010).** Life in blue: copper resistance mechanisms of bacteria and archaea used in industrial biomining of minerals. *Biotechnol Adv* **28**, 839–848.

**Reeve, J. N. (2003).** Archaeal chromatin and transcription. *Mol Microbiol* **48**, 587–598.

**Reiter, W. D., Hüdepohl, U. & Zillig, W. (1990).** Mutational analysis of an archaebacterial promoter: essential role of a TATA box for transcription efficiency and start-site selection *in vitro*. *Proc Natl Acad Sci U S A* **87**, 9509–9513.

**Robinson, N. J. & Winge, D. R. (2010).** Copper metallochaperones. *Annu Rev Biochem* **79**, 537–562.

**Rockabrand, D., Livers, K., Austin, T., Kaiser, R., Jensen, D., Burgess, R. & Blum, P. (1998).** Roles of DnaK and RpoS in starvation-induced thermotolerance of *Escherichia coli*. *J Bacteriol* **180**, 846–854.

**Rolfsmeier, M. & Blum, P. (1995).** Purification and characterization of a maltase from the extremely thermophilic crenarchaeote *Sulfolobus solfataricus*. *J Bacteriol* **177**, 482–485.

**Rolfsmeier, M., Haseltine, C., Bini, E., Clark, A. & Blum, P. (1998).** Molecular characterization of the alpha-glucosidase gene (malA) from the hyperthermophilic archaeon *Sulfolobus solfataricus*. *J Bacteriol* **180**, 1287–1295.

**Sambrook, J. & Russell, D. W. (2001).** *Molecular Cloning: A Laboratory Manual*, 3rd edn, vol. 2. Cold Spring Harbor, NY: Cold Spring Harbor Laboratory Press.

**Santangelo, T. J. & Reeve, J. N. (2006).** Archaeal RNA polymerase is sensitive to intrinsic termination directed by transcribed and remote sequences. *J Mol Biol* **355**, 196–210.

**Schelert, J., Dixit, V., Hoang, V., Simbahan, J., Drozda, M. & Blum, P. (2004).** Occurrence and characterization of mercury resistance in the hyperthermophilic archaeon *Sulfolobus solfataricus* by use of gene disruption. *J Bacteriol* **186**, 427–437.

**Schelert, J., Drozda, M., Dixit, V., Dillman, A. & Blum, P. (2006).** Regulation of mercury resistance in the crenarchaeote *Sulfolobus solfataricus*. *J Bacteriol* **188**, 7141–7150.

**Schué, M., Dover, L. G., Besra, G. S., Parkhill, J. & Brown, N. L. (2009).** Sequence and analysis of a plasmid-encoded mercury resistance operon from *Mycobacterium marinum* identifies MerH, a new mercuric ion transporter. *J Bacteriol* **191**, 439–444.

**Serre, L., Rossy, E., Pebay-Peyroula, E., Cohen-Addad, C. & Covès, J. (2004).** Crystal structure of the oxidized form of the periplasmic mercury-binding protein MerP from *Ralstonia metallidurans* CH34. *J Mol Biol* **339**, 161–171.

**Simbahan, J., Kurth, E., Schelert, J., Dillman, A., Moriyama, E., Jovanovich, S. & Blum, P. (2005).** Community analysis of a mercury hot spring supports occurrence of domain-specific forms of mercuric reductase. *Appl Environ Microbiol* **71**, 8836–8845.

**Sowers, K. R., Blum, P. H. & DasSarma, S. (2007).** Gene transfer in archaea. In *Methods for General and Molecular Microbiology*, 3rd edn, pp. 800–824. Edited by C. A. Reddy, T. J. Beveridge, J. A. Breznak, G. A. Marzluf & T. M. Schmidt. Washington, D.C.: American Society for Microbiology Press.

**Unniraman, S., Prakash, R. & Nagaraja, V. (2002).** Conserved economics of transcription termination in eubacteria. *Nucleic Acids Res* **30**, 675–684.

**Villafane, A., Voskoboynik, Y., Ruhl, I., Sannino, D., Maezato, Y., Blum, P. & Bini, E. (2011).** CopR of *Sulfolobus solfataricus* represents a novel class of archaeal-specific copper-responsive activators of transcription. *Microbiology* **157**, 2808–2817.

**Wang, Y., Boyd, E., Crane, S., Lu-Irving, P., Krabbenhoft, D., King, S., Dighton, J., Geesey, G. & Barkay, T. (2011).** Environmental conditions constrain the distribution and diversity of archaeal merA in Yellowstone National Park, Wyoming, U.S.A. *Microb Ecol* **62**, 739–752.

**Worthington, P., Hoang, V., Perez-Pomares, F. & Blum, P. (2003a).** Targeted disruption of the alpha-amylase gene in the hyperthermophilic archaeon *Sulfolobus solfataricus*. *J Bacteriol* **185**, 482–488.

**Worthington, P., Blum, P., Perez-Pomares, F. & Elthon, T. (2003b).** Large-scale cultivation of acidophilic hyperthermophiles for recovery of secreted proteins. *Appl Environ Microbiol* **69**, 252–257.

**Wright, K. J., Marr, M. T., II & Tjian, R. (2006).** TAF4 nucleates a core subcomplex of TFIID and mediates activated transcription from a TATA-less promoter. *Proc Natl Acad Sci U S A* **103**, 12347–12352.

Edited by: D. Nies